Available online at www.sciencedirect.com
ScienceDirect
Journal of the European Ceramic Society 27 (2007) 1935–1943
www.elsevier.com/locate/jeurceramsoc

Characterization of glass–alumina functionally graded coatings obtained by plasma spraying

V. Cannillo, L. Lusvarghi, C. Siligardi, A. Sola *

Dipartimento di Ingegneria dei Materiali e dell'Ambiente, University of Modena and Reggio Emilia, Via Vignolese 905, 41100 Modena, Italy

Received 3 February 2006; received in revised form 25 May 2006; accepted 31 May 2006
Available online 1 August 2006

Abstract

Glass–alumina functionally graded coatings (FGCs) were produced via plasma spraying, a deposition technique for thick (>10–20 μm) coatings production, which ensures high flexibility and good reliability. The samples were obtained by building a graded glass–alumina coating onto an alumina substrate; the coatings were designed as multi-layered systems, each layer having a mean composition slightly different from the neighbouring ones. Two different compositional gradients were considered (from 100 vol.% alumina to 100 vol.% glass and from 80–20 vol.% glass to 100 vol.% glass) and several heat treatments were performed in order to improve the substrate-coating interface and induce a controlled transformation (sintering and/or crystallization) of the glassy phase. After a preliminary screening of the as-sprayed and the heat treated samples, the most interesting ones were carefully characterized, especially from a mechanical point of view. In fact, tests such as Vickers micro-indentation allowed to appreciate the effects of the graded compositional profile and the consequences induced by thermal treatments.

Keywords: Microstructure-final; Mechanical properties; Al_2O_3; Glass; FGMs (functionally graded materials)

1. Introduction

Functionally graded materials (FGMs) are an innovative class of composite materials, characterized by a gradual variation of composition in space. In fact, unlike customary composite materials, the constituent phases of FGMs are not uniformly distributed in space, but are placed in order to create a gradual change in composition and therefore in properties and performances.[1,2] In this way it is possible to tailor the material microstructure to the assigned thermo-mechanical loading conditions and, in the meanwhile, the smooth compositional gradient avoids abrupt joints between heterogeneous materials, which can be detrimental in traditional bi-materials systems.[3–6] Moreover, the introduction of a functional gradient, if properly designed and realized, can confer special properties to the FGM, which can not be achieved by the FGM constituent phases considered separately or by the traditional composite material having the same mean composition as the FGM. For example, Suresh and co-workers[7] studied a glass–alumina FGM, obtained by means of percolation of a molten glass into a polycrystalline alumina substrate. The gradual variation of composition from a glass-rich superficial layer to a pure alumina substrate resulted into a smooth change in the elastic properties. The authors demonstrated that, under a spherical Hertzian indentation, the functional gradient induced a redistribution of the principal tensile stresses into the interior of the system, which in turn was able to suppress the formation of Hertzian cone cracks. On the contrary, Hertzian cracks were observed in bulk glass and alumina samples, and also in a composite system having the same mean composition as the FGM.

Recently, the concept of FGM has been promptly extended to several systems. However, in order to exploit its advantageous potentialities, the production of an FGM requires an adequate production technique, since the gradient should be realized in a controlled and well reproducible way.[2]

Thermal spraying has proved to be a flexible and reliable method to produce FGMs, mainly suitable for functionally graded coatings (FGCs). Basically, in thermal spraying the feedstock material, usually in powder form, is injected into a high pressure, high temperature gas flow, heated by an electric arc or the combustion of a gaseous or liquid fuel. In this way, the particles, while melting in the flame, are strongly accelerated

* Corresponding author. Tel.: +39 059 2056240; fax: +39 059 2056243.
E-mail address: sola.antonella@unimore.it (A. Sola).

0955-2219/$ – see front matter © 2006 Elsevier Ltd. All rights reserved.
doi:10.1016/j.jeurceramsoc.2006.05.105

towards the substrate, where they impinge, flatten and solidify very quickly (quenching).[1,8] Thermal spraying is an appealing approach, since it allows to deposit even really refractive coatings on less refractive substrates. Moreover a careful control of the spraying parameters and conditions enables to design the final composition and microstructure of the deposited system. This potentiality, therefore, is particularly favourable for the FGM production. On the other hand, the idea of grading the composition and microstructure of the sprayed coating may significantly improve the quality of the sprayed coatings with respect to traditional bi-material systems, for example by smoothing the abrupt connection between heterogeneous phases.[1,9–13]

In recent years, thermal spraying has been applied to three main classes of graded coatings. Thermal sprayed FGMs have been used as sensor and energy applications.[14] Moreover thermal spraying has emerged as an ideal technique to deposit thermal barrier coatings; actually this technique allows to spray highly thermally insulating ceramic coatings on metallic substrates, such as in gas turbines. Thermal sprayed functionally graded coatings have also been applied to industrial devices and machinery in order to enhance their superficial resistance against wear and erosion.[15,16] Since the coating durability may be reduced by microstructural defects, special post treatments have been developed to adjust the microstructure without altering the imposed gradient[17]; great attention has been devoted to the improvement of the bonding strength and to the reduction of possible thermal residual stresses.[18–24]

Up to date, however, the main topic of the research on thermal sprayed FGM is the understanding of the relation existing between process parameters, FGM microstructural features and macroscopic performances.[25] This is an ambitious target, since the characteristic microstructural features of thermal sprayed systems[26]—e.g. lamellar morphology, inter- and intra-lamellar pores and microcracks—are combined with the peculiar FGM spatial variation of composition and microstructure.

The present work was focused on the production of glass–alumina FGMs by plasma spraying. The FGMs were obtained by depositing a glass–alumina graded coating onto an alumina substrate. Two different glass–alumina gradients were considered: in the first type, the first layer deposited on the alumina substrate was made of pure alumina; in the second type, the first layer was made of 80 vol.% alumina and 20 vol.% glass. Moreover several thermal treatments were performed in order to induce a controlled sintering and/or crystallization of the glassy phase, thus obtaining new ceramic-glass ceramic FGMs. The resulting samples were investigated and compared.

2. Materials and methods

2.1. Ingredient materials

The substrate was made of a commercially available sintered alumina.[27] The alumina was a high density (3.9 g/cm^3)[27], pure (99.7%)[27] product, supplied in form of square tiles (50 mm × 50 mm × 8 mm). In order to gain a deeper insight into the substrate properties, an alumina specimen was observed with a scanning electron microscope (SEM – Philips XL-30) and the cross-section underwent an X-ray diffraction (XRD—X'Pert Pro PANalytical), which was required to define the crystal phases. Moreover the principal elastic properties of the alumina, i.e. Young's modulus and Poisson's coefficient, were measured via a resonance based technique (EMOD – Lemmens Grindosonic® MK5). Microindentation tests (Vickers Indenter, Open Platform, CSM Instruments) were performed by applying a load of 500 g_f for 15 s on the alumina cross-section in order to evaluate the Vickers hardness. A dilatometric analysis (NETZSCH – DIL 404) was carried out by heating an alumina sample from room temperature to 1400 °C; the mean value of the coefficient of thermal expansion was evaluated from room temperature to about 800 °C, which is the glass transition temperature of the glass used in the coating process.[28–30]

The graded coatings were built by spraying proper mixtures of alumina powder and glass powder. As regards the alumina, it was a commercial powder (Sulzer Metco 105SFP), characterized by a purity of 99.5% and a mean grain size of 31 ± 4 μm. A XRD was carried out on the alumina powder as well.

The glass used in the graded coatings belonged to the $CaO–ZrO_2–SiO_2$ (CZS) system, which was chosen for several reasons. First of all, the glasses belonging to this ternary system usually show interesting chemical and physical properties and remarkable mechanical performances (e.g. high Young's modulus and relatively good fracture toughness[28,29]). Furthermore, the glass composition could be formulated thus minimizing the mismatch in the coefficients of thermal expansion of the glass and the alumina used as substrate.[30] Moreover the glass formulation did not include Al_2O_3 and this circumstance was helpful to characterize the resulting systems, since the ingredient materials (alumina and glass) had completely different compositions.[29] Besides this, preliminary studies[28,29] proved that CZS glasses, if properly formulated, exhibit well defined and distinguished temperatures of sintering (about 850 °C) and crystallization (about 1050 °C) and therefore they are suitable for controlled heat-induced transformations. To conclude, CZS glasses (having compositions slightly different from the present one) have already been used with success to obtain plasma sprayed glass–alumina composites.[31,32]

The CZS glass used in this study was characterized in detail in a previous work.[29] In particular, in order to obtain the plasma sprayed FGMs, the glass was utilized in powder form. Accordingly, the raw materials (calcium carbonate, zirconium silicate, quartz) were mixed and melted, thus obtaining a molten glass which was plunged into cold water; the resulting glass frit was wet ball-milled and dried off in a kiln. The glass frit was subjected to an XRD to exclude the presence of residual, not perfectly fused crystal impurities. Moreover the glass was spray-dried in order to confer it a suitable flowability (NIRO Atomizer, Denmark – located at the Centro Sviluppo Materiali S.p.A., Roma).

2.2. Functionally graded materials

The FGMs were designed as multi-layered coatings which were plasma sprayed on the alumina square tiles. Within each layer the composition was (on average) uniform; in other words,

each layer could be theoretically considered as a traditional, not graded composite material.[1,33] Moving from the substrate-coating interface toward the upper surface, the mean content of alumina was decreased of 5 vol.% in each layer, while the mean content of glass was increased of 5 vol.%. In this way two different FGMs were produced, in the following named FGM1 and FGM2. In the former, the first layer sprayed on the alumina substrate was made of pure alumina; the second layer was made of 95 vol.% alumina and 5 vol.% CZS glass and so on, up to the top layer made of pure glass. In the former system, instead, the first layer deposited on the alumina substrate was made of 80 vol.% alumina and 20 vol.% glass. In both types of FGMs, the layer thickness was minimized and it was kept constant (around 30 μm).

Spray runs were carried out by using a F4-MB plasma torch installed in a Controlled Atmosphere Plasma-Spraying plant at Centro Sviluppo Materiali S.p.A. (Roma, Italy), which is co-shared with the University "La Sapienza" (Roma). Both FGM1 and FGM2 were realized in APS mode, applying the operating parameters that are listed in Table 1. The alumina substrates were previously grit blasted at Centro Sviluppo Materiali S.p.A. using a vacuum-operated Norblast blasting machine equipped with a hand-held blasting gun (internal diameter 8 mm). SiC particles[34] with a mean grain size of 165 μm were employed as grits. Moreover the alumina substrates were slightly pre-heated up to about 150 °C.

A traditional, well established method to obtain plasma sprayed FGMs consists in pre-mixing the spraying powders in various ratios and then depositing individual layers by spraying the previously blended mixtures of powders.[35–38] In the present research, instead, the spraying powders (alumina; atomized CZS glass) were not pre-mixed: they were separately loaded in two different powder feeders and the graded profile was built by gradually varying the feeding flow rate of the powders into the plasma flux.[39] In order to define the feeding rate of each powder, a deposition efficiency measurement was previously performed: the alumina powder and the glass one were separately sprayed on a substrate of known thickness by fixing the same spraying parameters and the same number of torch passes; then the thickness of each coating was measured and the ratio between the two thicknesses was used to calibrate the corresponding feeding rates. The feeding parameters are listed in Table 2.

Table 2
Feeding parameters for the FGCs

Glass % in the layer	Feeding disk speed (rpm)	
	Glass	Alumina
0[a]	0.0	25.0
5[a]	0.3	24.7
10[a]	0.7	24.3
15[a]	1.1	23.9
20	1.5	23.5
25	1.9	23.1
30	2.4	22.6
35	3.0	22.0
40	3.6	21.4
45	4.3	20.7
50	5.1	19.9
55	5.9	19.1
60	6.9	18.1
65	8.0	17.0
70	9.3	15.7
75	10.8	14.2
80	12.6	12.4
85	14.7	10.3
90	17.4	7.6
95	20.7	4.3
100	25.0	0.0

[a] Layers deposited only in FGM1 and not in FGM2.

In order to induce the sintering and/or crystallization of the glassy phase in the FGMs, several thermal treatments were attempted, which can be grouped in two families:

- Single isotherm. The heating cycle included the following steps: heating from 25 to 500 °C at 5 °C/min; heating from 500 °C to the maximum temperature at 10 °C/min; 30 min isotherm at the maximum temperature; slow cooling down to room temperature. In different heat treatments, the maximum temperature was set to 850 °C (heat treatment labeled as 850), 950 °C (labeled as 950), 1050 °C (labeled as 1050), 1500 °C (labeled as 1500) and 1600 °C (labeled as 1600).
- Double isotherm. The heating cycle included the following steps: heating from 25 to 500 °C at 5 °C/min; heating from 500 to 850 °C at 10 °C/min; 30 min isotherm at 850 °C; heating from 850 °C to 1050 °C at 10 °C/min; 30 min isotherm

Table 1
Plasma torch operating parameters

	FGM1	FGM2
Torch type	F4-MB, internal diameter: 6 mm	F4-MB, internal diameter: 6 mm
Power	550 A × 71 V = 39050 W	550 A × 71 V = 39050 W
Spraying distance	100 mm	100 mm
Number of passes	3 pre-heating + 40 spraying	3 pre-heating + 28 spraying
	Carrier gas 1: Ar, 3.5 slpm	Carrier gas 1: Ar, 3.5 slpm
	Carrier gas 2: Ar, 3.5 slpm	Carrier gas 2: Ar, 3.5 slpm
Powder injection system	Injector axial distance from torch exit: 7 mm	Injector axial distance from torch exit: 7 mm
	Injector angular distance from torch exit: 90°	Injector angular distance from torch exit: 90°
	Injector internal diameter: 1.8 mm	Injector internal diameter: 1.8 mm
Plasma gas composition and flow	Ar, 45 slpm; H_2 14 slpm	Ar, 45 slpm; H_2 14 slpm
Cooling system	Cooling gas: Ar pressure 8 bar	Cooling gas: Ar pressure 8 bar
Substrate temperature during deposition	About 150 °C	About 150 °C

at 1050 °C; slow cooling down. This thermal treatment was labeled as DI.

The temperatures were chosen on the basis of the thermal behaviour of the glass, which sinters at about 850 °C and crystallizes at 1050 °C, as shown in previous works.[28,29]

The final FGMs, both as-sprayed and heat treated, were cut along the gradient direction; the cross-section of each specimen was carefully polished and observed through the SEM, in order to evaluate its microstructure. Moreover each type of FGM underwent a XRD (on the coating surface), which was needed to identify the crystal phases developed during the plasma spraying and/or the thermal treatment (if performed). These preliminary tests allowed to identify the most interesting samples, which were more carefully characterized and, if required, compared with the original alumina used as substrate. The cross-section of each selected FGM underwent several Vickers indentations performed along lines parallel to the alumina-coating interface; the maximum load of 100 g_f was applied for 15 s. This test was intended to evaluate the mean Vickers hardness as a function of depth (i.e. as a function of the distance from the upper surface), which was representative of the functional gradient associated with the compositional gradient. The deep abrasion resistance of the surface (Ceramic Instruments AP/87 abrasimeter) was evaluated via a dry particle abrasion test. During the test, a flux of alumina particles (FEPA 80, having a mean diameter of 180 μm) flows tangentially to a rotating steel disk which, in the meanwhile, is pressed by a fixed load against the specimen surface. Since the tested FGMs showed a different coating thickness, they could bear a different number of disk revolutions before the coating was removed. Therefore, in order to obtain comparable results, the abraded volume was normalized by the total distance L (in m) covered by the disk, i.e. $L = 2\pi rN$, where r is the disk radius and N is the number of cycles. The results were expressed as normalized volume V_n (in mm^3/m). The scratch tests (Open Platform, CSM Instruments) were performed on the top surface of the specimens with a Rockwell diamond indenter (radius 200 μm) and the measure schedule included two progressive scratches (from 1 to 30 N, with a loading speed of 14.5 N/min), which were useful to define a critical load, i.e. the load at which a severe damage in the coated system could be easily detected by an optical microscope; the critical load, therefore, was defined in a qualitative way and was just intended as a mean of comparison between the analysed samples. After identifying the critical load, two multi-pass scratches and two single-pass scratches were performed at a sub-critical load. Each scratch line was 1 mm long.

3. Results and discussion

3.1. Ingredient materials

The SEM inspection of the alumina substrates revealed a polycrystalline microstructure, with some residual closed porosity in the cross-section (about 6 vol.%). Thanks to the XRD, only one crystal phase could be detected, i.e. rhombohedral-structured Al_2O_3 (α alumina).

The Young's modulus and Poisson's ratio of the bulk alumina resulted to be 379.2 GPa and 0.21, respectively. The microhardness, measured via Vickers indentations, was $HV_{500g_f} = 1587 \pm 111$. The dilatometric analysis gave a value of the coefficient of thermal expansion equal to $8.28\,10^{-6}\,K^{-1}$.

The alumina powder employed in the functionally graded coatings underwent an XRD and its spectrum resulted to be qualitatively the same as the substrate one, revealing the presence of a rhombohedral-structured Al_2O_3.

The CZS glass frit, at the end of the wet ball-milling, was extremely fine, as revealed by the granulometric analysis (monomodal trend, with D50 at about 14 μm and D90 at about 40 μm) and therefore, in order to enhance its attitude to flow through the feeding apparatus, it was spray-dried to get hollow particles of about 30–50 μm in size, composed by the finer glass powder. The XRD excluded any relevant survival of not molten raw materials.

3.2. Functionally graded materials

The SEM inspection of the as-sprayed FGM cross-sections confirmed that the designed compositional gradients were accurately realized. FGM1 (Fig. 1a), whose planned gradient varied from 100 vol.% alumina to 100 vol.% glass, was reasonably thicker than FGM2 (Fig. 1b), whose imposed gradient spanned from 80 vol.% alumina – 20 vol.% glass to 100 vol.% glass, being their thickness around 700 and 500 μm, respectively. In both samples, the individual splats of each ingredient material were clearly distinguishable. Though the microstructure morphology was mainly lamellar, in some areas the glass phase was poorly flattened keeping a round shape typical of a partially molten glass droplet (Fig. 1a and b, arrows). The authors have already verified such behaviour with sprayed glasses having both similar[32] and very different compositions[40] to the one used here. Possible proposed explanations could be found in the glass low thermal conductivity, in its relatively high viscosity at high temperatures with respect to a previously crystalline molten material and the relatively low velocity acquired by the glass in the flame due to its low density (<3.0 g/cm^3).[28]

The SEM images proved that in the sprayed coatings it was not possible to identify neighbouring layers characterized by different mean compositions. Actually, the mean thickness of each planned layer was around 30 μm and therefore it was comparable with the characteristic microstructural unit size of the system, represented by the splat dimension.[1,33] This means that, even if the graded coatings were designed as multi-layered FGMs, the fabricated coatings could be considered as continuous FGMs. However, the continuous gradient of FGM1 and FGM2 was the overall result of an intrinsically discrete and stochastic distribution of the ingredient materials at the microscale, since the alumina splats and the glass ones remained separate domains (Fig. 2). Though the sprayed materials are heterogeneous at the microscale, in the as-sprayed samples the interface between the two phases was very regular and it did not show major defects. This peculiarity was caused by the gradual change of the glass viscosity during the splat quenching, which allowed the glass lamellae to fit the alumina roughness.

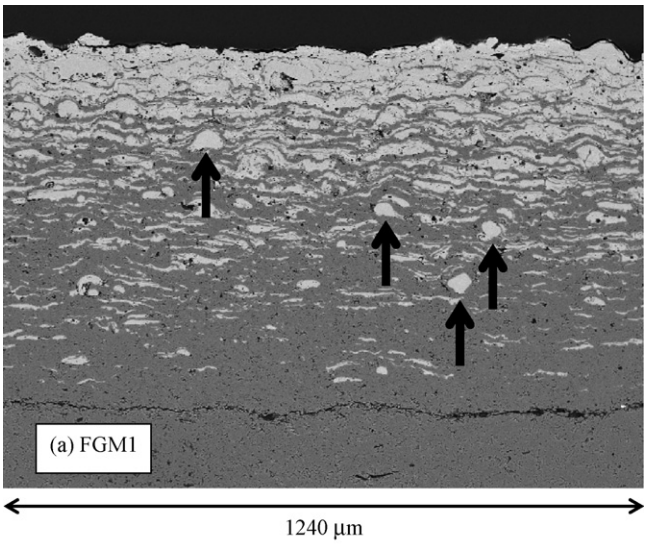

Fig. 1. SEM images of the as-sprayed FGM1 (a) and FGM2 (b) cross-sections. Some round-shaped glass domains can be seen (arrows).

The graded coatings were relatively compact, with a fine, uniformly dispersed porosity. The porosity of the glass top layer can be considered closed and mainly not interconnected; nevertheless some cracks, caused by the abrupt quenching of the splats or, in general, by the release of the thermal stresses, can be detected. The alumina phase is characterized by the typical irregular interconnected porosity of highly refractive oxides ceramic coatings obtained by plasma spraying.

The XRD of the cross-section of the as-sprayed samples revealed the presence of two alumina polymorphs: a rhombohedral Al_2O_3 (α alumina) and a cubic Al_2O_3 (γ alumina).

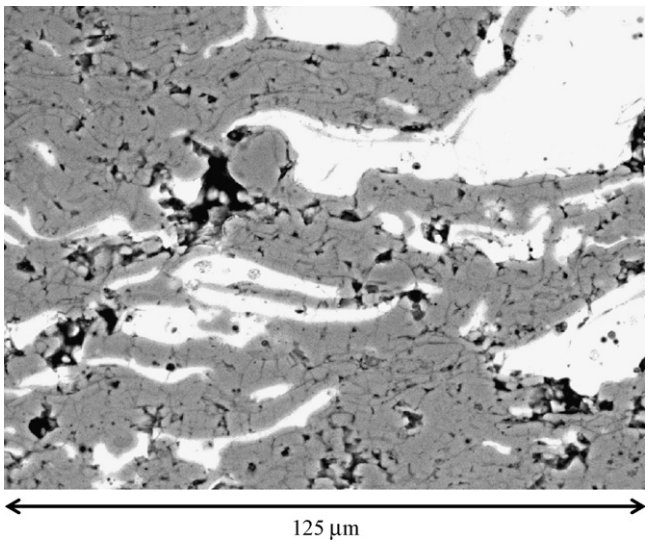

Fig. 2. Microstructural heterogeneity of the sprayed FGMs (detail of the FGM1 cross-section).

The former was identified with the alumina of the substrate or some sprayed alumina particles not completely molten during the deposition; the latter was caused by the polymorphic transformation of the alumina powder during the plasma spraying process. The diffraction analysis, repeated on the top surface of the samples, showed that the glass was the only phase existing in the coatings surface.

One major problem of the as-sprayed FGMs was the substrate-coating interface, which resulted to be defective though the substrate had previously been grit blasted and the ingredient materials had been chosen in order to minimize the thermo-mechanical mismatch. Several thermal treatments, which also caused the sintering and/or crystallization of the glass, were tried in order to enhance the substrate-coating interface.

The results of the thermal treatments, as observed by SEM (coupled with XRD, if required), are summarized in Table 3. The effects of the heat treatments on the FGCs were consistent with the thermal behaviour of the glass,[28,29] since the employed CZS glass sinters at around 850 °C and crystallizes at around 1050 °C, with the development of wollastonite as main phase. As a consequence, the heat treatment at 850 °C induced a good sintering of the glass, while the isothermal step at 1050 °C allowed the glass crystallization. The samples heated to 950 °C underwent a partial sintering (the temperature was too high) and a partial crystallization (the temperature was too low).

It is worth noting that in FGM1-SI-1050 and FGM1-DI the graded coating completely exfoliated at the end of the cooling

Table 3
Effect of thermal treatments on plasma sprayed FGMs

System	Temperature (°C)			
	850	950	1050	850 + 1050
FGM1	Sintered	Partially sintered + poorly crystallized	Crystallized delaminated	First sintered, then crystallized delaminated
FGM2	Sintered	Partially sintered + poorly crystallized	Crystallized	First sintered, then crystallized

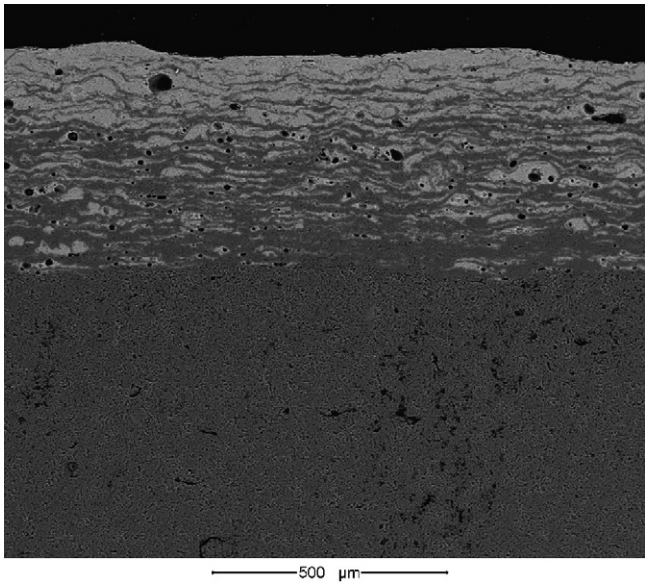

Fig. 3. Cross-section of the sample FGM2-DI.

down, while in FGM2-SI-1050 and FGM2-DI the graded coating adhered perfectly to the alumina substrate. This remarkably dissimilar behaviour was caused by the difference in thickness and compositional gradient. As already said, in fact, the FGM1 samples were characterized by a thicker coating than the FGM2 samples and therefore they experienced higher post-deposition stresses which were likely to be not completely relaxed during the thermal treatment; furthermore, they underwent more severe stresses during the thermal treatment itself and the glass crystallization.[41] Moreover in the FGM1 samples the first layer deposited on the alumina substrate was made of pure alumina, while in the FGM2 samples the first layer contained a significant glass volume fraction, and it is reasonable stating that at 1050 °C some glass was molten, thus acting as a matching agent with the substrate.

As regards the samples treated at 1500 and 1600 °C, as expected, the temperature was too high and the heat treated coatings resulted extremely porous and deformed, mainly because of the heated air entrapped by a wide crystallization. Moreover the development of anorthite and gehlenite suggested that the alumina and the glass chemically interacted.

On the basis of these considerations, some interesting systems were identified: FGM1, FGM1-SI-850 (sintered glass), FGM2, FGM2-DI (sintered and crystallized glass, Fig. 3). These samples, together with the bulk alumina substrate, were more accurately investigated. The Vickers indentation tests, which were performed on the cross-section of the FGM specimens, revealed that the hardness progressively increased as a function of depth, thus confirming that the compositional gradient resulted in a property gradient (Fig. 4). This was a reasonable result, since the alumina Vickers hardness (1587 ± 111 Vickers, see previous section) was higher than the glass one (670 ± 59 Vickers[29]) and the alumina amount became progressively greater as a function of depth. On average, after the thermal treatment both FGM1 and FGM2 experienced an increase in Vickers hardness. However, the benefits were especially evident in FGM2, since it was possible to sinter and subsequently crystallize the glass, while in FGM1 the glass could be only sintered. Moreover the improvement was particularly relevant in those regions of the cross-sections which were rich in glass. Actually in the deeper regions of the FGM1 cross-section, that were extremely rich in alumina, the Vickers hardness was not bettered by the thermal treatment; on the contrary, in FGM2 the Vickers hardness of the deeper regions was significantly improved, thanks to their relatively high glass content (not lower than 20 vol.%). As a matter of fact, during the thermal treatment the alumina thermomechanical properties were not radically modified (even if the γ alumina re-transformed in α alumina[42]); on the contrary, the glass sintering in FGM1-SI-850 and its sintering and crystallization in FGM2-DI led to a remarkable enhancement of the mechanical performances, at least at a microscale level.

The beneficial effect of the thermal treatment was confirmed by the deep abrasion tests (Fig. 5). At a fixed number of cycles, the normalized volume of abrasion was much lower for the heat treated sample than for the as-sprayed one, due to the sintering and, in case, crystallization of the glass. Moreover, in the as-sprayed FGM2 sample, the alumina substrate was exposed to view by the coating removal after 100 cycles. However, after the thermal treatment, the coating-substrate interface was not reached any more. It is worth noting that, being the number of cycles the same, the normalized volume of abrasion was

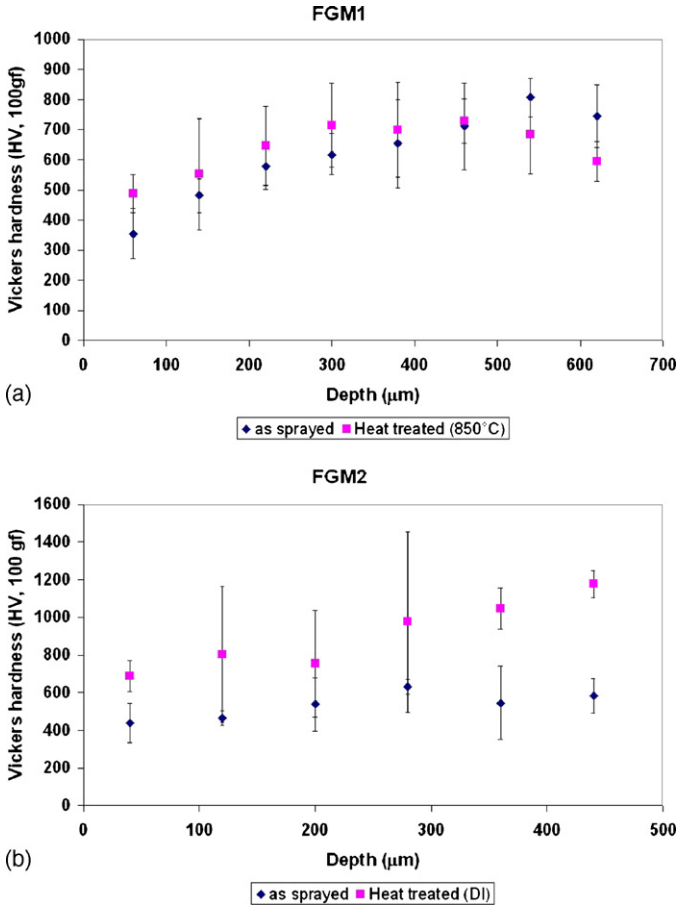

Fig. 4. Effect of the thermal treatment on the Vickers hardness in FGM1 (a) and FGM2 (b).

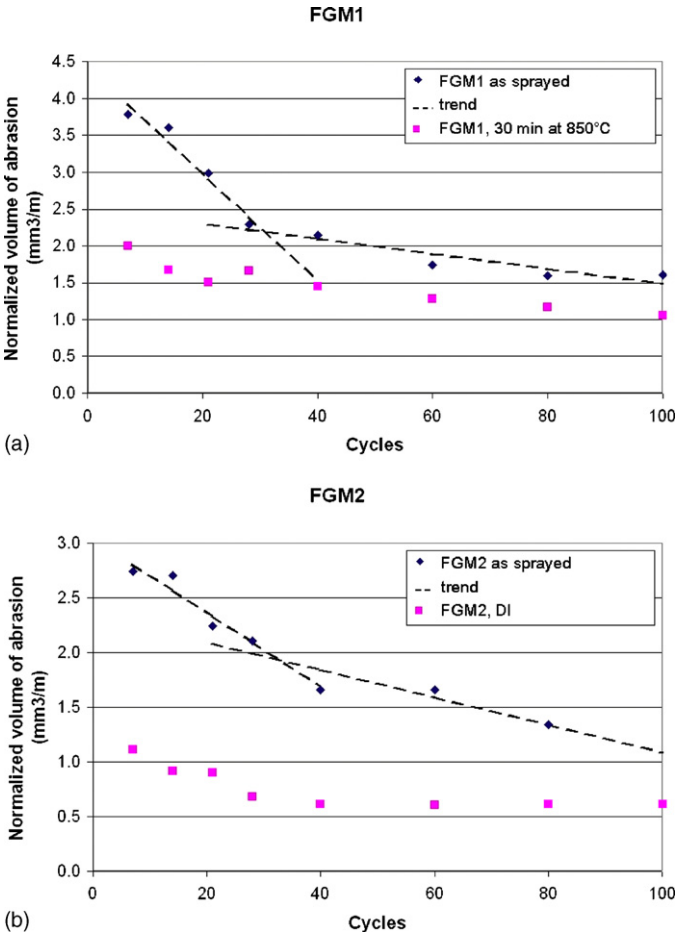

Fig. 5. Effect of the thermal treatment on the abrasion resistance.

systematically lower for FGM2 than for FGM1. In fact, it is likely that the FGM2 sample, which generally showed a higher coating-substrate adhesion and a lower stress state (potentially better cohesion between "layers"), could reach a higher resistance to the deep abrasion. It should be underlined that the normalized volume of abrasion of the as-sprayed FGMs diminished as a function of the number of cycles, but the rate of decrease was really quick up to about 30 cycles, then it became much smoother (see dashed lines in Fig. 5a and b). This may suggest that the most superficial area, which was rich in glass, could be easily removed, but, if a certain alumina volume fraction was reached (about 50%), the FGM resistance to abrasion became very good. Then, even if the alumina volume fraction further increased (in fact at increasing depths the alumina percentage was higher and higher), the resistance was not significantly improved. Instead, after the thermal treatment, the normalized volume of abrasion decreased gradually thus suggesting that the FGM behaviour varied in a really smooth way along the gradient direction, demonstrating a much better cohesion between the two phases, along with a substantial reinforcement of the glass thanks to its sintering and crystallization.

The advantage of performing a thermal treatment could be qualitatively appreciated during the scratch test as well. First of all, the scratch tracks were much more evident in the as-sprayed specimens than in the heat treated ones, especially in FGM2. Moreover the critical load, defined by means of the progressive scratch test, was increased by the thermal treatment. As regards the FGM2, for example, the sintering and subsequent crystallization raised the critical load from 4 to 15 N, a value which was comparable with the alumina one. Fig. 6 presents a direct comparison between the tracks induced by a multi-pass scratch test (4×) with a load of 15 N on the top surfaces of the pure alumina bulk (Fig. 6a) and the FGM2-DI sample (Fig. 6b). The SEM observation of the scratch tracks showed that, if the load was high enough, the coatings – both as-sprayed and heat treated – underwent two concurrent failure mechanisms, i.e. backward brittle cracking and peeling failure (Fig. 7). The advancing indenter induces compressive plastic deformation on the very surface because it produces a hydrostatic stress state.[43] After the indenter passage, the elastic recovery leaves a tensile stress state and for this reason some areas can undergo a backward (tensile) cracking

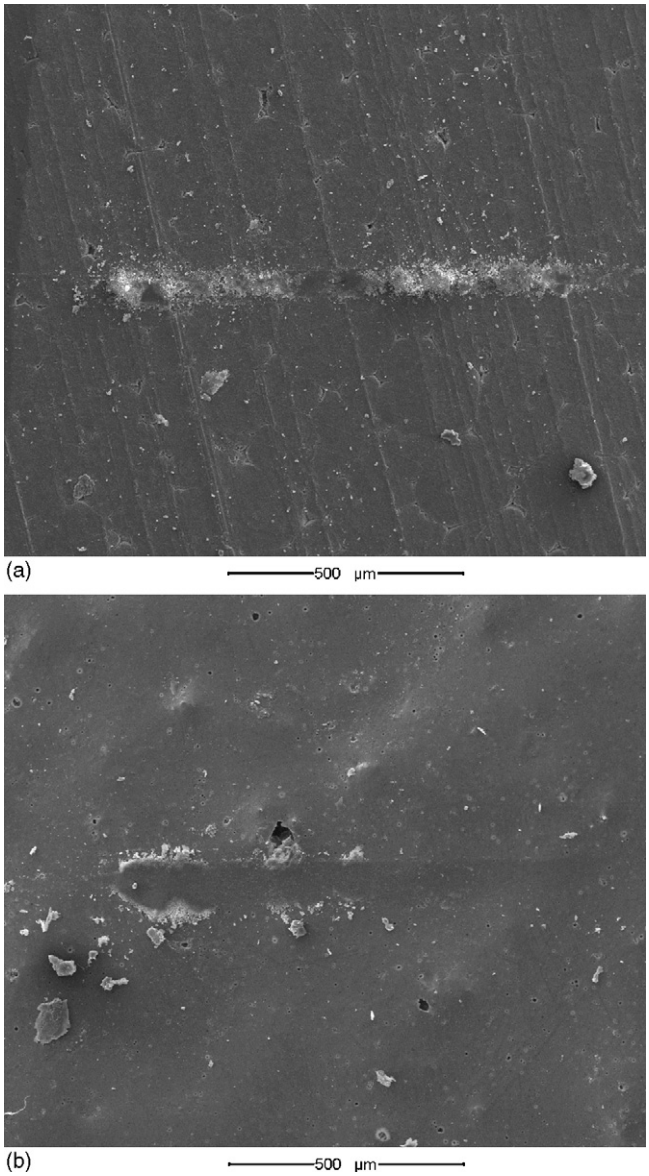

Fig. 6. Comparison between the multi-pass scratch test (four passes; 15 N load) on the top surfaces of the alumina bulk (a) and the FGM2-DI sample (b).

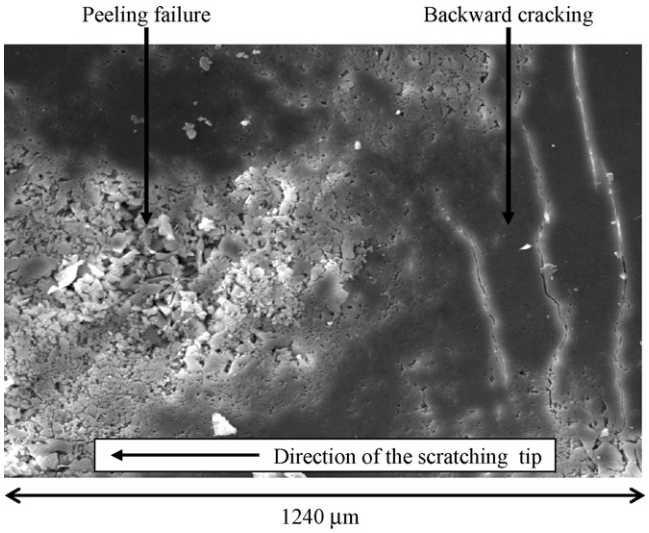

Fig. 7. Failure mechanisms coexisting in the analysed systems during scratch test (detail of progressive scratch track in FGM2 as-sprayed).

phenomenon, as deduced by the crack paths.[44] When the load is high enough, the hertzian stresses acting below the surface can cause subsuperficial brittle cracking, allowing the surface top layers to be peeled off. Besides, the mismatch between the strains in the plastically deformed surface and the underlying elastically deformed material engenders interfacial stresses which favours delamination.[43] In the peeling failure mode, areas where wear debris – caused by the underling brittle cracking – are flattened and embedded in the bottom of the track by the indenter stylus are clearly visible. It is worth noting that, once more, the sample FGM2 showed higher superficial performances, especially after the thermal treatment, because of the controlled sintering and crystallization of the glassy phase.

4. Conclusions

The present investigation proved the feasibility of glass–alumina functionally graded materials by plasma spraying. Actually, this production technique proved to be reliable, since the designed compositional gradients could be faithfully realized; moreover, a careful setting of the spraying parameters enabled to control the final composition and microstructure which, in turn, governed the system performances.

The FGMs were deposited as multi-layered coatings, but the minimization of the layers thickness allowed to obtain a continuous gradient, since in the final samples it was not possible to distinguish the single layers. The microstructure, however, was locally heterogeneous, since the glass and the alumina splats were clearly identifiable.

The major problem with the as-sprayed samples was their relatively defective microstructure and interface between the graded coating and the alumina substrate. Hence, a proper thermal treatment was performed in order to improve the cohesion and adhesion. In fact, the thermal treatment, if properly engineered, could result in the sintering and/or crystallization of the glassy phase of the graded coating. In particular, if the graded coating composition ranged from pure alumina (next to the alumina substrate) to pure glass, it was possible to sinter the glass, but not to crystallize it, since the coating underwent a delamination due to the thermo-mechanical mismatch between the newly formed phases and the alumina. On the contrary, if the coating composition already included some glass next to the interface, it was possible to sinter and then to crystallize the glassy phase without any delamination. The different behaviour of the examined FGMs during the thermal treatment was likely to be due to the different thickness of the coatings and, most of all, to the presence or absence of the glass next to the interface. In fact the glass, if present, favoured the adhesion of the coating. The mechanical tests proved that the thermal treatment, if properly performed, was advantageous, leading to a sensible improvement of the superficial performances of the glass–alumina FGM: both the resistance to scratching and to dry particle abrasion were substantially increased.

Acknowledgements

The present research was partially supported by PRRIITT (Regione Emilia Romagna), Net-Lab "Surface & Coatings for Advanced Mechanics and Nanomechanics" (SUP&RMAN). Centro Sviluppo Materiali (CSM) S.p.A. (Roma, Italy), Surface Engineering Unit, is gratefully acknowledged for the spraying sessions. Many thanks to Ing. Giovanni Bolelli (Dipartimento di Ingegneria dei Materiali e dell'Ambiente, Università di Modena e Reggio Emilia, Italy) for his precious help in the coating design.

References

1. Miyamoto, Y., Kaysser, W. A., Rabin, B. H., Kawasaki, A. and Ford, R. G., *Functionally Graded Materials. Design, Processing and Applications*. Kluwer Academic Publishers, 1999.
2. Kawasaki, A. and Watanabe, R., Concept and P/M fabrication of functionally graded materials. *Ceram. Int.*, 1997, **23**, 73–83.
3. Becker, T. L., Cannon, R. M. and Ritchie, R. O., Statistical fracture modelling: crack path and fracture criteria with application to homogeneous and functionally graded materials. *Eng. Frac. Mech.*, 2002, **69**, 1521–1555.
4. Rabin, B. H. and Shiota, I., Functionally Gradient Materials. *MRS Bullet.*, 1995, **XX**(1), 14–15.
5. Koizumi, M. and Niino, M., Overview of FGM research in Japan. *MRS Bullet.*, 1995, **XX**(1), 19–21.
6. Schulz, U., Peters, M., Bach, Fr.-W. and Tegeder, G., Graded coatings for thermal, wear and corrosion barriers. *Mater. Sci. Eng. A.*, 2003, **362**, 61–80.
7. Jitcharoen, J., Padture, N. P., Giannakopoulos, A. E. and Suresh, S., Hertzian-crack suppression in ceramics with elastic-modulus-graded surfaces. *J. Am. Ceram. Soc.*, 1998, **81**(9), 2301–2308.
8. Handbook of Thermal Spray Technology, In J.R. Davis ed., Davis and Associates, ASM International 2004.
9. Sampath, S., Herman, H., Shimoda, N. and Saito, T., Thermal spray processing of FGMs. *MRS Bullet.*, 1995, **1**, 27–31.
10. Wan, Y. P., Sampath, S., Prasad, V., Williamson, R. and Fincke, J. R., An advanced model for plasma spraying of functionally graded materials. *J. Mater. Process. Technol.*, 2003, **137**(1–3), 110–116.
11. Kawasaki, A. and Watanabe, R., Thermal fracture behavior of metal/ceramic functionally graded materials. *Eng. Frac. Mech.*, 2002, **69**(14–16), 1713–1728.
12. Khor, K. A. and Gu, Y. W., Effects of residual stress on the performance of plasma sprayed functionally graded ZrO_2/NiCoCrAlY coatings. *Mater. Sci. Eng. A*, 2000, **277**(1–2), 64–76.

13. Khor, K. A., Dong, Z. L. and Gu, Y. W., Plasma sprayed functionally graded thermal barrier coatings. *Mater. Lett.*, 1999, **38**(6), 437–444.
14. Müller, E., Drašar, Č., Schilz, J. and Kaysser, W. A., Functionally graded materials for sensor and energy applications. *Mater. Sci. Eng. A*, 2003, **362**(1–2), 17–39.
15. Prchlik, L., Sampath, S., Gutleber, J., Bancke, G. and Ruff, A. W., Friction and wear properties of WC-Co and Mo-Mo_2C based functionally graded materials. *Wear*, 2001, **249**(12), 1103–1115.
16. Zhao, H. X., Yamamoto, M. and Matsumura, M., Slurry erosion properties of ceramic coatings and functionally gradient materials. *Wear*, 1995, **186–187**(2), 473–479.
17. Stewart, S., Ahmed, R. and Itsukaichi, T., Contact fatigue failure evaluation of post-treated WC-NiCrBSi functionally graded thermal spray coatings. *Wear*, 2004, **257**(9–10), 962–983.
18. Widjaja, S., Limarga, A. M. and Yip, T. H., Modeling of residual stresses in a plasma-sprayed zirconia/alumina functionally graded-thermal barrier coating. *Thin Solid Films*, 2003, **434**(1–2), 216–227.
19. Pan, C. and Xu, X., Microstructural characteristics in plasma sprayed functionally graded ZrO2/NiCrAl coatings. *Surf. Coat. Technol.*, 2003, **162**(2–3), 194–201.
20. Khor, K. A. and Gu, Y. W., Thermal properties of plasma-sprayed functionally graded thermal barrier coatings. *Thin Solid Films*, 2000, **372**(1, 2), 104–113.
21. Dong, Z. L., Khor, K. A. and Gu, Y. W., Microstructure formation in plasma-sprayed functionally graded NiCoCrAlY/yttria-stabilized zirconia coatings. *Surf. Coat. Technol.*, 1999, **114**(2–3), 181–186.
22. Khor, K. A., Dong, Z. L. and Gu, Y. W., Plasma sprayed functionally graded thermal barrier coatings. *Mater. Lett.*, 1999, **38**(6), 437–444.
23. Fu, L., Khor, K. A., Ng, H. W. and Teo, T. N., Non-destructive evaluation of plasma sprayed functionally graded thermal barrier coatings. *Surf. Coat. Technol.*, 2000, **130**(2–3), 233–239.
24. Kesler, O., Matejicek, J., Sampath, S., Suresh, S., Gnaeupel-Herold, T., Brand, P. C. *et al.*, Measurement of residual stress in plasma-sprayed metallic, ceramic and composite coatings. *Mater. Sci. Eng. A*, 1998, **A257**(2), 215–224.
25. Ilschner, B., Processing-microstructure-property relationships in graded materials. *J. Mech. Phys. Solids*, 1996, **44**(5), 647–656.
26. Wang, Z., Kulkarni, A., Deshpande, S., Nakamura, T. and Herman, H., Effects of pores and interfaces on effective properties of plasma sprayed zirconia coatings. *Acta Mater.*, 2003, **51**, 5319–5334.
27. Kéramo ceramiche tecniche, Tavernerio (CO), Italy.
28. Leonelli, C. and Siligardi, C., CaO-SiO_2-ZrO_2 glasses: modelling and experimental approach. *Recent Res. Develop. Mater. Sci.*, 2002, **3**, 599–618.
29. Cannillo, V., Manfredini, T., Siligardi, C. and Sola, A., Glass-alumina functionally graded materials: their preparation and compositional profile evaluation. *J. Eur. Ceram. Soc.*, 2006, **26**(13), 2685–2693.
30. Cannillo, V., de Portu, G., Micele, L., Montorsi, M., Pezzotti, G., Siligardi, C. and Sola, A., Microscale computational simulation and experimental measurement of thermal residual stresses in glass-alumina Functionally Graded Materials. *J. Eur. Ceram. Soc.*, 2006, **26**(8), 1411–1419.
31. Bolelli, G., Lusvarghi, L., Manfredini, T. and Siligardi, C., Influence of the manufacturing process on the crystallization behavior of a CZS glass system. *J. Non-Cryst. Solids*, 2005, **351**(30–32), 2537–2546.
32. Bolelli, G., Cannillo, V., Lusvarghi, L., Manfredini, T., Siligardi, C., Bartuli, C. *et al.*, Plasma-sprayed glass-ceramic coatings on ceramic tiles: microstructure, chemical resistance and mechanical properties. *J. Eur. Ceram. Soc.*, 2005, **25**(11), 1835–1853.
33. Mortensen, A. and Suresh, S., Functionally graded metals and metal-ceramic composites. II. Thermomechanical behaviour. *Int. Mater. Rev.*, 1997, **42**(3), 85–116.
34. Zamboni Luciano, Montichiari (BS) ITALY (Provider).
35. Gu, Y. W., Khor, K. A., Fu, Y. Q. and Wang, Y., Functionally graded ZrO_2-NiCrAlY coatings prepared by plasma spraying using pre-mixed, spheroidized powders. *Surf. Coat. Technol.*, 1997, **96**, 305–312.
36. Xiang, X., Zhu, J., Yin, Z. and Lai, Z., Fabrication and microstructure of ZrO_2/NiCrCoAlY graded coating by plasma spraying. *Surf. Coat. Technol.*, 1996, **88**, 66–69.
37. Khor, K. A., Gu, Y. W. and Dong, Z. L., Plasma spraying of functionally graded yttria stabilized Zirconia/NiCoCrAlY coating system using composite powders. *J. Thermal Spray Technol.*, 2000, **9**(2), 245–249.
38. Dianran, Y., Jining, H., Xiangzhi, L., Yangai, L., Yanchun, D. and Hai, L., The corrosion behavior of plasma-sprayed Ni/Al–Al_2O_3 and Ni/Al–Al_2O_3 + 13 wt.% TiO_2 graded ceramic coatings in 5%HCl solution. *Surf. Coat. Technol.*, 2003, **176**, 30–36.
39. Vaidya, R. U., Castro, R. G., Peters, M. I., Gallegos, D. E. and Petrovic, J. J., Use of plasma spraying in the manufacture of continuously graded and layered/graded molybdenum disilicide/alumina composites. *J. Therm. Spray Technol.*, 2002, **11**(3), 409–414.
40. Bolelli, G., Cannillo, V., Lusvarghi, L. and Manfredini, T., Glass-alumina composite coatings by plasma spraying. Part I: microstructural and mechanical characterization, *Surf. Coat. Technol.,* in press.
41. Godoy, C., Souza, E. A., Lima, M. M. and Batista, J. C. A., Correlation between residual stresses and adhesion of plasma sprayed coatings: effects of a post-annealing treatment. *Thin Solid Films*, 2002, **420–421**, 438–445.
42. Damani, R. J. and Wanner, A., Microstructure and elastic properties of plasma-sprayed alumina. *J. Mater. Sci.*, 2000, **35**, 4307–4318.
43. Xie, Y. and Hawthorne, H. M., The damage mechanisms of several plasma-sprayed ceramic coatings in controlled scratching. *Wear*, 1999, **233-235**, 293–305.
44. Burnett, P. J. and Rickerby, D. S., The relationship between hardness and scratch adhesion. *Thin Solid Films*, 1987, **154**, 403–416.